Learning-based systems for assessing hazard places of contagious diseases and diagnosing patient possibility

Davoodi Monfared, M.; Ghaffari, M.;

Originally published:

October 2022

Expert Systems With Applications 213(2023)1, 1

DOI: https://doi.org/10.1016/j.eswa.2022.119043

Perma-Link to Publication Repository of HZDR:

https://www.hzdr.de/publications/Publ-35381

Learning-based Systems for Assessing Hazard Places of Contagious Diseases and Diagnosing Patient Possibility

Mansoor Davoodi[a,b,c] (mdmonfared@iasbs.ac.ir), Mohsen Ghaffari[a,d] (mohsen.ghaffari@iasbs.ac.ir)

[a] Department of Computer Science and Information Technology, Institute for Advanced Studies in Basic Sciences, Zanjan, Iran

[b] Center for Advanced Systems Understanding (CASUS), D-02826 Görlitz, Germany

[c] Helmholtz-Zentrum Dresden-Rossendorf (HZDR), Dresden, 10 01328, Germany

[d] Department of Computer Science, IT University of Copenhagen, Copenhagen, 2300, Denmark

Corresponding Author:

Mansoor Davoodi

Department of Computer Science and Information Technology, Institute for Advanced Studies in Basic Sciences, Zanjan, Iran

Tel: +98 24 3315–3376

P.O. Box: 45137-66731

Email: mdmonfared@iasbs.ac.ir

Abstract

To manage the propagation of infectious diseases, particularly fast-spreading pandemics, it is necessary to provide information about possible infected places and individuals, however, it needs diagnostic tests and is time-consuming and expensive. To smooth these issues, and motivated by the current Coronavirus disease (COVID-19) pandemic, in this paper, we propose a learning-based system and a hidden Markov model (i) to assess hazardous places of a contagious disease, and (ii) to predict the probability of individuals' infection. To this end, we track the trajectories of individuals in an environment. For evaluating the models and the approaches, we use the Covid-19 outbreak in an urban environment as a case study. Individuals in a closed population are explicitly represented by their movement trajectories over a period of time. The simulation results demonstrate that by adjusting the communicable disease parameters, the detector system and the predictor system are able to correctly assess the hazardous places and determine the infection possibility of individuals and cluster them accurately with high probability, i.e., on average more than 96%. In general, the proposed approaches to assessing hazardous places and predicting the infection possibility of individuals can be applied to contagious diseases by tailoring them to the influential features of the disease.

Keywords: Machine Learning, Trajectory Tracking, Patient Prediction, Hidden Markov Model, Covid-19, Trajectory Clustering

1. Introduction

Efficiently managing contagious diseases needs online and updated information about infected peoples and hazardous places. For unknown viruses such as the fast-spreading severe acute respiratory syndrome coronavirus 2 (SARS-CoV-2) and the related disease, coronavirus disease 2019 (COVID-19), finding a pattern of transmission and spreading in a short period is not possible. Thus,

the key managing advice of the World Health Organization (WHO) is to perform more tests and isolating the positive cases (https://www.who.int/director-general/speeches/detail/who-director-general-s-opening-remarks-at-the- media-briefing-on-covid-19—16-march-2020). While, the test capacity in the countries, particularly for developing countries is limited, and consequently, preventing the epidemic outbreak and controlling and managing the propagation of them are so difficult. To smooth this issue, in this paper we develop efficient learning-based systems using the movement trajectories of the individuals whose diagnostic status is known (or will be known soon) and diagnose the hazardous places of a city. Further, by having such information and movement trajectories of people, it is possible to determine the probability of an individual being infected.

So, in this paper, we focus on the following research questions:

1. Where are the infected places of a contagious disease in a city?, and, How much is each place infected?
2. How much is the patient possibility for a person who moves around a city?

To answer these questions, we first accommodate the required inputs. That is, we introduce a structure which makes it easy to work with the dynamic environment of the problem. Then, we introduce two learning-based systems; one learns the hazardous possibility of each place, and one explores the trajectory tracking of an individual and computes the patient likelihood via a hidden Markov model (HMM)-based approach. To this end, we gather the movement information of a group of people in a city. We compute a disease hazardous probability for each place and find risky places. Then, by investigating the moving trajectory of a new (given) individual, we predict the probability of he/she being infected.

Both the proposed learning systems are general frameworks with inputs that can be customized for communicable diseases by setting propagation parameters such as transmission rate and convalescence. In this paper, we incorporate Covid-19's infection and propagation parameters. The systems provide useful information from the contaminated places in a city and the infection rate of individuals whose movement trajectories are available. Such information is very

practical in establishing and updating social and personal protocols to manage and control the disease. Further, the results provided by the predictor system can be efficiently utilized in pooling approaches, that is, grouping a set of individuals in one pool and perform a test on the combined samples of them (Mutesa et al., 2020). Such approaches are very time and cost-saving if the pools contain a few infected individuals (Escobar et al., 2020). So, it is very helpful if the people with a high probability of prevalence are tested individually and the people with low prevalence probability are tested in groups. The approach proposed in this paper provides such prevalence probabilities for the individuals whose movement history is available.

In this paper, we suggest a detector system to assess the hazardous places of a contagious disease in a city by using a supervised learning-based approach on the individuals' tracking trajectories. To obtain the individuals' trajectories, we use the GPS information of a set of volunteers walking around a city. The detector system can set up on a warning mobile device to notify the hazardous places. Furthermore, we propose a predictor system, which predicts the possibility of getting the disease without testing. The state-based nature of the predictor system's issues such as having uncertain knowledge about a person who does not a diagnostic test, a sequential behavior of a person in the environment, local observing in the environment, permanently transmission to patient state, and probabilistic transmission from a state to another one are the reasons that have convinced us to propose an HMM-based approach to develop such predictor system.

It is notable, in recent years mobile computing and mobile technology are now more connected, sophisticated, location-based, personal, and powerful than ever. Positioning technologies that serve mobile phones such as the cellular antenna, global navigation satellite systems and GPS, and the Wi-Fi positioning system provide increasingly accurate and continuous geographic positions of mobile devices. So, it is easy to track the location of a massive number of mobile devices. We know that because of security and privacy issues, some people do not allow access to their location all the time in a period. However,

the proposed system would handle it if they let to have their movement paths partially for a while. Also, it only requires the individuals' trajectories without knowing the ID of the persons.

This paper is organized into six sections. In the next section, the state of the art in the relevant area is reviewed. Preliminaries and definitions are introduced in the section 3. Section 4 explains the proposed approaches in this paper. Section 5 includes the results of applying the proposed method on Covid-19 cases and the analysis of the research results. Finally, Section 6 concludes the paper and presents future work.

2. Related Work

Machine Learning (ML) approaches have been significantly used to design detection and prediction systems (Ghaffari & Afsharchi, 2020). Detection systems extract features of a phenomenon, like a disease, and detect the possibility of occurring by having some observations and witnesses. Prediction systems are used to predict the progression of the phenomenon and its impact on different aspects. Since some features may are observable and some are hidden, the pattern of phenomena can be used for both the detection and prediction systems. Consequently, ML approaches that learn based on the patterns allow us to study both observed features (e.g., a patient with symptoms of a disease) and hidden features (e.g., an infected person without symptoms of a disease).

Several ML-based approaches for automatic detection of communicable diseases such as Covid-19 have been suggested utilizing X-ray and Computer Tomography (CT) images (Ismael & Şengür, 2020; Apostolopoulos & Mpesiana, 2020; Gozes et al., 2020; Li et al., 2020a; Wang et al., 2020; Wynants et al., 2020). Also, prognostic prediction approaches based on ML algorithm and Markov model (MM) have been proposed (Choudhury et al., 2020; Yan et al., 2020; Roda et al., 2020). Randhawa et al. (2020) combined supervised ML with digital signal processing for genome analyses, augmented by a decision tree approach to the ML component, and a Spearman's rank correlation coefficient

analysis for result validation. Ahamad et al. (2020) developed a supervised ML-based method to identify the presentation features predicting Covid-19 disease. They examined features such as details of the individuals concerned, e.g., age, gender, observation of fever, history of travel, and clinical details such as the severity of cough and incidence of lung infection. There are also studies on predicting the progression of Covid-19 using MM (Atkeson, 2020; Liu et al., 2020). Rao & Vazquez (2020) introduced a recognition system based on several ML predictive models to explore the impacts of Covid-19 on people's mental health. Ong et al. (2020) applied the Vaxign reverse vaccinology and Vaxign-ML tools to predict Covid-19 vaccine candidates. Tian & Zhang (2020) assessed the performance of three ML models including HMM, hierarchical Bayes model, and long-short-term-memory model (LSTM) to show a predictive model of the disease would help allocate medical resources and determine social distancing measures more efficiently. Li et al. (2020b) hypothesized that Deep Learning (DL) approaches might be able to extract Covid-19's specific graphical features and provide a clinical diagnosis ahead of the pathogenic tests, thus they save critical time for disease control. Perez & Dragicevic (2009) developed an agent-based modeling approach that integrates geographic information systems (GIS) to simulate the spread of a communicable disease in an urban environment, as a result of individuals' interactions in a geospatial context.

Recently, deep neural networks have shown remarkable performance in the analysis of sequential data. Irio & Oliveira (2021) compared two innovative methodologies to predict the future locations of moving vehicles when their current and previous locations are known. They used two methodologies based on the Bayesian network to infer the statistics of prior vehicles, trajectory data that is further adopted in the estimation process, and a deep learning approach based on Recurrent Neural Networks (RNNs). Priyanka et al. (2021) used Covid-19 time-series datasets, and with the help of deep learning, they suggested the model for predicting confirmed positive, recovered and mortality of Covid-19 cases. They developed a prediction model using RNN in the first instance, and subsequently, the second model was built using Long Short Term Memory

Networks (LSTMs).

Ismael & Şengür (2020) suggested DL-based approaches to classify Covid-19 and healthy chest X-ray images. The proposed methods have been used deep feature extraction, fine-tuning of pretrained convolutional neural networks (CNN), and end-to-end training of a developed CNN model. Apostolopoulos & Mpesiana (2020) suggested a DL-based method for the automatic detection of the Coronavirus, utilizing a dataset of X-ray images from patients with common bacterial pneumonia, confirmed Covid-19 disease, and normal incidents. They detected various abnormalities in small medical image datasets by using transfer learning. Li et al. (2020a) developed a DL model, Covid-19 detection neural network, to extract visual features from volumetric chest CT exams for the detection of Covid-19. Gozes et al. (2020) presented a system that utilizes robust 2D and 3D deep learning approaches, modifying and adapting existing artificial intelligence (AI) models and combining them with clinical understanding, to develop automated CT image analysis tools for detection, quantification, and tracking of Coronavirus. The developed system can differentiate coronavirus patients from those who do not have the disease. Wang et al. (2020) demonstrated that non-identifiability in model calibrations using the confirmed-case data was the main reason for wide variations of predictions on the Covid-19 epidemics.

Atkeson (2020) introduced an MM of the progression of Covid-19 in the United States. This model allows for quantitative statements regarding the trade-off between the severity and timing of suppression of the disease through social distancing and the progression of the disease in the population. Liu et al. (2020) reviewed the basic reproduction number (R_0) of the Covid-19 by using a stochastic Markov chain. They illustrated that R_0 estimation depends on the estimation method used as well as the validity of the underlying assumptions. Yan et al. (2020) built a prognostic prediction model based on the XGBoost ML algorithm to predict the mortality risk and presented a clinical route to the recognition of critical cases from severe cases. Choudhury et al. (2020) created a decision-analytic Markov state transition model to simulate the life of critically

ill Covid-19 patients as they transitioned to either recovery or death. Rao & Vazquez (2020) sampled and analyzed the Weibo posts using the approach of *online ecological recognition* based on several ML predictive models. They explored the impacts of Covid-19 on people's mental health to assist policymakers to develop actionable policies and help clinical practitioners, e.g., social workers, psychiatrists, and psychologists.

There are also several studies on predicting disease progression using various DL approaches. Hernandez-Matamoros et al. (2020) proposed models to predict the evolution of Covid-19 epidemic by analyzing different geographical areas. Alaa & Schaar (2018, 2019) developed the phased attentive state space (PASS) model of disease progression, a deep probabilistic model that captures complex representations for disease progression while maintaining clinical interpretability. Unlike Markovian state-space models, which assume memoryless dynamics, PASS uses an attention mechanism to induce "memoryful" state transitions, whereby repeatedly updated attention weights are used to focus on past state realizations that best predict future states. Joint models to forecast disease trajectories longitudinal over time suffer from limitations that arise from a fixed model specification and computational difficulties when applied to high-dimensional datasets. Lim & Schaar (2018) proposed a deep learning approach to address these limitations, enhancing existing methods with the inherent flexibility and scalability of deep neural networks while retaining the benefits of joint modeling. Pham et al. (2017) introduced DeepCare, an end-to-end deep dynamic neural network that reads medical records, stores previous illness history, infers current illness states and predicts future medical outcomes. At the data level, DeepCare represented care episodes as vectors and models patient health state trajectories by the memory of historical records. Bueno et al. (2019) proposed a probabilistic framework based on HMM for predicting disease dynamics guided by latent states.

Further, several studies have suggested probabilistic generative models and providing individualized predictions of future disease progression.Fong et al. (2020) developed an approach using Composite Monte-Carlo, which is enhanced

by DL network and fuzzy rule induction for gaining better stochastic insights about the epidemic development. Futoma et al. (2016) proposed a probabilistic generative model to provide individualized predictions of future disease progression while jointly modeling the pattern of related recurrent adverse events. They fitted their model using a scalable variational inference algorithm. Galagali & Xu-Wilson (2018) presented an approach to subtype irregular patient data while acknowledging the underlying progression of disease states. Their approach consists of two components: a probabilistic model to determine the likelihood of a patient's observation trajectory and a mixture model to measure the similarity between asynchronous patient trajectories. Kumar (2020) introduced a method to collect large amounts of diagnostic data about cognitive processes in short periods of testing. The method is demonstrated by a task assessing an individual's use of attention and motor control. Nagesh et al. (2019) modeled and predicted longitudinal glaucoma measurements using an interpretable, discrete state space model. They presented a technique for incorporating spatio-temporal the retinal nerve fiber layer thickness measurements obtained from a sequence of OCT images into a longitudinal progression model. Neyja et al. (2017) presented an Internet of Things (IoT)-based health care system implementation scheme using HMM chain and ElectroCardioGram sensors within the context of e-Health. Vairavan et al. (2012) proposed an algorithm based on logistic regression and HMM using vital signs, laboratory values and fluid measurements to develop an improved patient-specific prediction of in-hospital mortality. Xiang et al. (2015) presented a framework to predict potential risks for medical conditions as well as its progression trajectory to identify the comorbidity path. The framework utilizes patients' publicly available social media data and presents a collaborative prediction model to predict the ranked list of potential comorbidity incidences, and a trajectory prediction model to reveal different paths of condition progression. Wang et al. (2022) proposed ARIMA, SARIMA and Prophet models to predict daily new cases and cumulative confirmed cases in the USA, Brazil and India over the next 30 days based on the COVID-19 new confirmed cases and cumulative confirmed cases data set. Chumachenko et al. (2022) developed

three statistical ML models for predicting the dynamics of the COVID-19 epidemic process. Further, they studied and compared effectiveness of the models not only for COVID-19 but also for other infectious diseases.

HMM is a helpful technique for trajectory tracking systems such as recognition of complex object motion trajectories, and eye-tracking (Bashir et al., 2005; Kim et al., 2020). Saini et al. (2020) used a genetic framework to choose the optimal set of features for trajectory classification. Although the treatment of most infectious diseases are known for medical scientists, and the transmission ways and rate for the viruses are identified, there are a few recent emerging diseases (such as Covid-19), which are unknown. In such cases, reverse engineering is one of the recognition solutions, which obtain by studying disease impact on society. Note that most of the previous studies in the literature have suggested their approach for a specific disease. Since transmission of an infectious disease may occur through several (but similar) pathways; through contact with infected individuals, by water, airborne inhalation, through the vector-borne spread, etc., we can develop a generalized solution to overwhelm the similar challenges. The other reason is diagnostic testing problems, such as being expensive, time-consuming, unreliable answers, and need to repeat. Therefore, we introduce two systems, to provide infection information and hazardous rate of different places of an environment, and to predict the probability of an individual being infected.

3. Preliminaries and Definitions

In this paper, we propose two systems; the detector system to assess hazard places, and the predictor system to predict the infected probability of an individual by having his/her trajectory. Both the systems work based on the movement trajectories of individuals in an environment like a city. We use a graph to model the environment, a geometric path to model the trajectories, and a layered data structure to consider the time in the real world. Table 1 includes all the symbols used in this paper.

Table 1 Symbols and Definitions

Symbol	Definition
$G = (V, E)$	Corresponding graph of a city
V	Set of vertices in G which include public places, hospitals, gas stations, etc.
E	Set of edges in G which illustrates connection between the neighbors
$\mathcal{P}$	Set of patients
p	A patiant individual $p \in \mathcal{P}$
$\mathcal{H}$	Set of healthy individuals
h	A healthy individual $h \in \mathcal{H}$
$\mathcal{U}$	Set of people whose healthy or patient status is not known
u	$u \in \mathcal{U}$
m	$m \in \mathcal{P} \cup \mathcal{H} \cup \mathcal{U}$
$\mathcal{T}_{(m,t)}$	The location of an individual m at time t
δ	The latent period (day)
$\mathcal{A}_P(p)$	The possibility of exposure of a virus in a place from a patient p
μ_i	The i^{th} (effective in infection or spreading) parameter of disease
$\phi(\mu_i)$	The probability function of μ_i in $\mathcal{A}_P(p)$
$\mathcal{R}_P(h)$	Possibility of reducing exposure of a virus in a place from a healthy individual h
$\theta(\mu_i)$	The probability function of μ_i in $\mathcal{R}_P(h)$
$\mathcal{G}_P(m)$	The possibility of getting the disease for an individual m
$\omega(\mu_i)$	The probability function of μ_i in $\mathcal{G}_P(m)$
l	A place in the modeled city
$\mathcal{S}_t(l)$	The hazardous rate of l at time t
n	Number of time slots
Q	Set of states of HMM
A	Transition probability matrix of HMM
O	Sequence of observations of HMM
B	Sequence of observation likelihoods of HMM
π	Initial probability distribution over states of HMM
α_t	Patient possibility of u at time slot t
d	Notation for day
ρ_d	The robability of an individual remains healthy after d days
σ	Personal hygiene
β	Patient ratio
C	A constant number
γ	Social distance
o	Specific infection parameters of Covid-19

Let $G = (V, E)$ be a corresponding graph of a city, where V is the set of vertices (places in a city) that contains apartments, hospitals, bus and train stations, shopping and sporting centers, etc. and E be the set of edges (the connection between the places). G is assumed an unweighted graph because the proposed systems learn based on the trajectories which represent the time that an individual travels or stays in a connection or a place. Figure 1a illustrates *Sareyn* city and Figure 1b demonstrates its corresponding extracted graph from its map. Figures 1c and 1d illustrate ten *healthy individuals* and ten *patient individual* trajectories in the city, respectively. The precision of modeling may

change using two parameters: the number of nodes in the graph, and the number of samples from the location of an individual in a period of time. Clearly, there is a trade-off between the complexity of the models and these two concepts. Although it is a challenge, we do not discuss it in this paper, and only focus on the detector and predictor systems.

Figure 1 (a) Sareyn city's map, (b) corresponding graph, (c) trajectories of 10 patients, and (d) trajectories of 10 healthy individuals (Davoodi & Ghaffari, 2021).

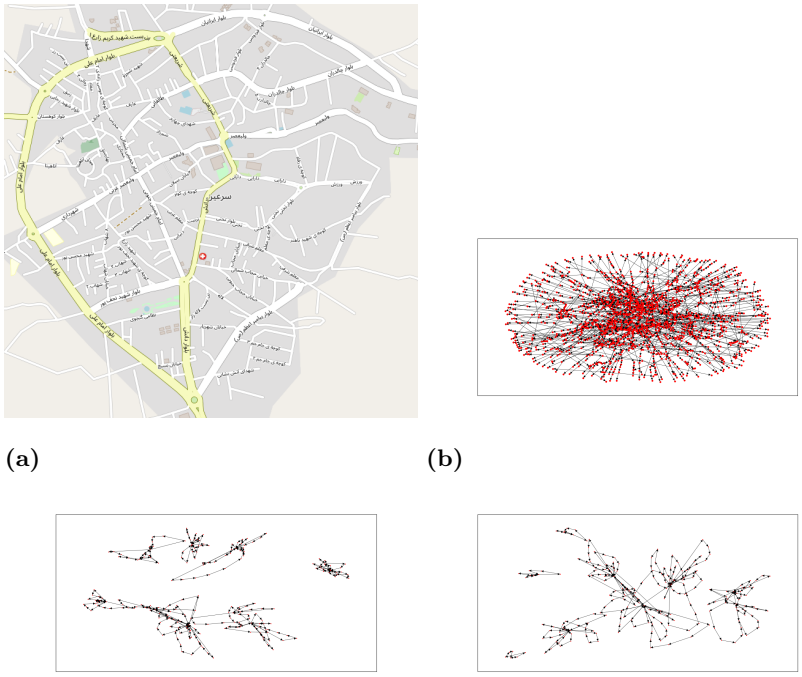

(a) **(b)**

(c) **(d)**

Formally, a *trajectory* is a curved path of an object follows after it is thrown or shot into the air, or of an object that is traveling through space (https:// dictionary.cambridge.org/dictionary /english/trajectory). So, it is a proper modeling tool for mapping the traveling paths which depend on time. In this paper, we consider a trajectory as a traveling path of a person through each time slot.

Let function $\mathcal{T}_{(m,t)}$ shows the location of person m at time slot t. Also, we suppose three categories of individuals:

- $\mathcal{P}$ is the set of individulas who are patient, e.g., their diagnostic test answer is positive
- $\mathcal{H}$ is the set of healthy individuals, e.g., their diagnostic test answer is negative
- $\mathcal{U}$ is the set of individuals whose health status is unknown

Each infection disease has several specific properties such as transmission possibility and transmission ways, period of impact of the virus, appearing time of symptoms, curative period (if there is), etc. In this paper, we consider the following assumptions.

- δ days needs to appear the disease symptoms,
- The starting time of the suffering is not recognizable,
- There is no surly curative,
- It is possible to recognize the patient by diagnostic tests.

We handle the second assumption using a probabilistic function, so we can relax it easily in case that the starting time of the suffering is known. A place does not have a self-potential to make hazard itself, but rather the patients make the place hazardous. On the other hand, certain predicting of people's behavior is not possible, so the environment is dynamic and stochastic. Finding features in common for these environments is a big challenge, and sometimes it is impossible. Therefore, we suggest a method that works based on the environment's state. Accordingly, when we call the hazard probability of a place, that is one or more infected individuals stayed there for some time slots.

Disease transmission is divided into two parts; spread of the virus by a host, and getting the disease by a healthy individual. The possibility of propagation of a virus in a place from the host depends on several parameters such as the

transition rate of the disease, personal hygiene, social distance and inattention to the antiseptic area. Accordingly, exposure from a patient $p \in \mathcal{P}$ is determined by:

$$\mathcal{A}_P(p) = \prod_{i=1}^{k} \phi(\mu_i), \tag{1}$$

where $\phi(\mu_i)$ is the probability function of ith (effective) parameter in infection and it may have a constant, linear, polynomial, exponential, or geometric distribution. Note that not only the parameters and their effect change from one disease to another one but also those would have diverse behaviors. Finding these parameters and the corresponding functions are professional issues and need medical experts, however, to focus on the objective in this paper, we just use and apply findings and improvements on the disease.

As it is expected, the hazardous rate of a place increases by entering some patients at that place. Also, it decreases when a healthy individual enters into that place and remain healthy for a while. So, the place should be less hazardous than what does learn by Eq (1). In other words, when some people go into a hazardous place, we expect that they get infected with a high probability. Now if we know they remain healthy, we find out the place was not as hazardous as we have expected. So, we decrease the hazardous probability of the place and update it by the following equation.

$$\mathcal{R}_P(h) = \prod_{i=1}^{k'} \theta(\mu_i), \tag{2}$$

where $\theta(\mu_i)$ is the probability function of ith parameter.

Let $\mathcal{G}_P(m)$ be the probability of an individual $m \in \mathcal{H} \cup \mathcal{U}$ being infected at the place P. In addition to presence in a hazardous place, various parameters such as hygiene and social distance have an impact on infection. $\omega(\mu_i)$ is the probability function of the i^{th} parameter, and $\mathcal{G}_P(m)$ is calculated by multiplying $\omega(\mu_i)$ for $i = 1, 2, ..., k''$. Note that, if parameter μ_i is to avoid getting sick (such as hygiene), we will multiply $1 - \omega(\mu_i)$ in the following equation.

$$\mathcal{G}_P(m) = \prod_{i=1}^{k''} \omega(\mu_i). \tag{3}$$

In this section, we introduced a general model of spreading and infecting functions. Also, we explained how to formulate the inputs of the proposed systems. As we mentioned, for adjusting a disease to the model, we need to define parameters ϕ, θ, and ω. In the next section, we describe the proposed systems.

4. The Detector and Predictor Systems

The predictor system is applied to determine the infection possibility of an individual whose moving trajectory is available. This system requires information about the hazardous probability of each place in the city. To provide this information, we first develop the detector system, which learns the hazardous probability of all the sampled places by using tracking of trajectories of patients (positive test individuals) and healthy individuals (negative test individuals). Figure 2 presents a visual representation of the methodology used in this study

The moving paths of people in a city are continuous in both terms of time and location. We apply a discrete model in both the terms, that is a graph represents the city and a set of sequential time slots. Indeed, it is difficult to model a trajectory without losing any information, however, by increasing the number of nodes in the graph and the number of time slots in a fixed period of time, we can increase the precision of modeling, however, these also increase the complexity. Therefore, there is a trade-off between the precision of modeling and its complexity. Regarding the scale of the city, the number of trajectories and computational resources, such trade-off can be handled properly. Similarly, the risk rate of a place varies over time. In fact, there is useful information on the life-time of viruses on different kinds of material and surfaces, and in general, the hazardous rate of a place decreases over time if no patient visits it. To incorporate this fact, we use a *layered data structure*. Each layer has information about the current state of the places in the city. Figure 3 illustrates

Figure 2 The methodology of Detector and Predictor Systems

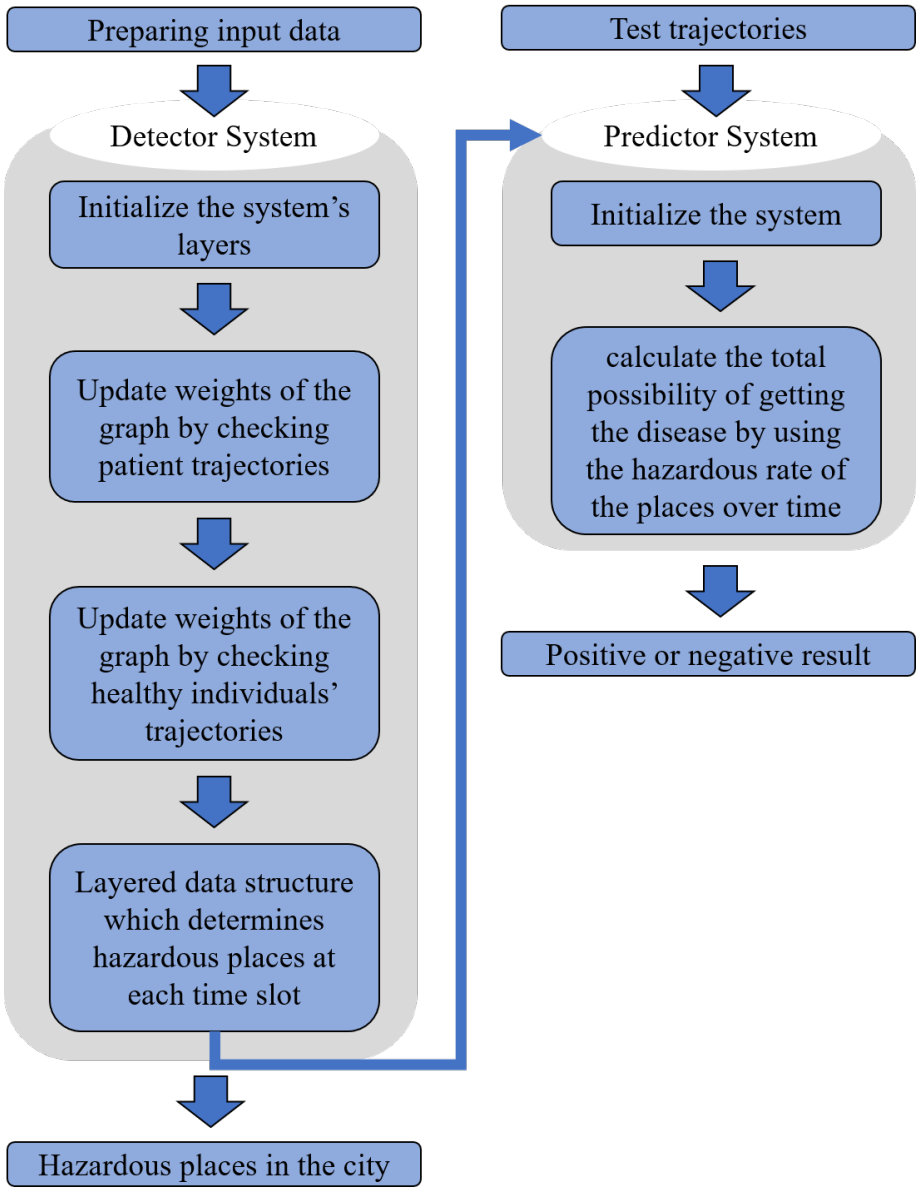

mapping a trajectory into the layered data structure. The points in the layers include not only the time and location of the individual but also the hazardous rate of the places.

Figure 3 A schematic view of layered data structure

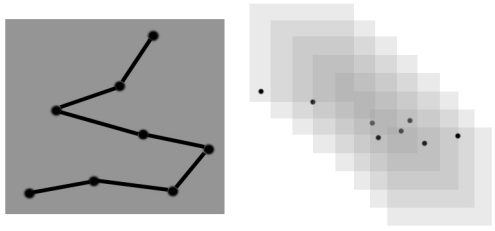

The detector system is developed based on the following observations.

Observation 1. *The hazard probability of a place increases when a patient visits it.*

Observation 2. *The hazard probability of a place decreases when a healthy individual visits it and remains healthy.*

Let $G = (V, E)$ be the corresponding graph of a city. To detect hazardous places, first, we construct a layered data structure $\mathcal{S}$ such that each layer contains all nodes in V, and each node has a label that is initialized to zero (refers to the hazard probability of each node at the first time slot). The number of layers depends on the precision factor as discussed above, and also the properties of the disease. Next, we update the hazard probability of places by using the trajectories of the individuals who already their diagnostic test's result are available. To this end, we consider the current time as the source of time and go back to the past step by step at each time slot. We start with the first layer (the first time slot), and investigate all people's places and update the hazardous

rate of the places. Then, we iteratively do this process for all the layers. Note that, we first handle the patient trajectories and then healthy ones. According to observation 1, the trajectory of a patient $p \in \mathcal{P}$ updates the hazardous of a place l at time slot t by:

$$\mathcal{S}_t(l) = 1 - ((1 - \mathcal{S}_t(l)) \times (1 - \mathcal{A}_P(p))). \tag{4}$$

Similarly, according to observation 2, each healthy individual $h \in \mathcal{H}$ updates the hazardous rate of l by:

$$\mathcal{S}_t(l) = \mathcal{S}_t(l) \times \mathcal{G}_P(h). \tag{5}$$

We apply all the trajectories of patients and healthy individuals to construct $\mathcal{S}_t$. It includes the hazard probability of each place in the city at time t. The proposed detector system determines hazardous places at each time slot, so, we can easily extend it to a day or a long period of time, and we can daily update the knowledge of the system. We keep the framework of the system simple as presented. This allows it easily is customized for different infectious diseases and is applied for large scale graph instances.

To design the predictor system, we propose an HMM. It utilizes the constructed layered structure $\mathcal{S}$ by the detector system. In general, an HMM allows studying on both observed events and hidden events that affect probabilistic phenomena. In our predictor system, the trajectory of a given unknown individual is a sequential observation for the HMM. So, the predictor system uses the places which the individual has visited until the current layer. It calculates the total possibility of getting the disease by using the hazardous rate of the places over time. Note that, if δ days need the disease symptoms appear, and each day includes n time slots, $\delta \times n$ layers is required to predict the patient possibility.

An HMM is specified by quintuplet $\{Q, A, O, B, \pi\}$, which Q is the set of states, A is the transition probability matrix (the probability of moving from one state to another one), O is the sequence of observations (the input sensing of the environment), B is the sequence of observation likelihoods (the probability

Figure 4 Illustration of the proposed HMM.

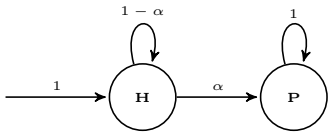

of an observation being generated from a state), and π is the initial probability distribution over the states (the probability that Markov chain starts in that state). In the proposed HMM (see Figure 4), we have

- $Q = \{\mathbf{H},\ \mathbf{P}\}$,
- $A = \begin{array}{c} \\ \mathbf{H} \\ \mathbf{P} \end{array} \begin{array}{c} \begin{array}{cc} \mathbf{H} & \mathbf{P} \end{array} \\ \begin{pmatrix} 1-\alpha & \alpha \\ 0 & 1 \end{pmatrix} \end{array}$,
- $O = \mathcal{S}_1(\mathcal{T}_{(u,1)}), \mathcal{S}_2(\mathcal{T}_{(u,2)}), \ldots, \mathcal{S}_n(\mathcal{T}_{(u,n)})$,
- $B = 1$,
- $\pi = \begin{array}{c} \begin{array}{cc} \mathbf{H} & \mathbf{P} \end{array} \\ \begin{pmatrix} 1 & 0 \end{pmatrix} \end{array}$,

where $u \in \mathcal{U}$, and $\alpha_t = \mathcal{S}_t(\mathcal{T}_{(u,t)}) \times \mathcal{G}_P(u)$ is the patient possibility of u at time slot t. Consequently, the probability of being health after a day d is

$$\rho_d = \prod_{t=1}^{n}(1-\alpha_t), \tag{6}$$

and the possibility that u has got the disease up to the current time slot T is:

$$\rho_T = \prod_{d=1}^{\delta}(1-\rho_d). \tag{7}$$

Although it is possible to extend the models to consider more parameters and states, here we tried to keep the models simple with low complexity. Despite the simplicity of the models, the simulation results confirm both them have high performance.

Theorem 1. *The detector system works in $O(|\mathcal{P} \cup \mathcal{H}|.n.\delta)$ time.*

Proof. Since the detector system uses all the trajectories of patient and healthy individuals once, it takes $|\mathcal{P} \cup \mathcal{H}|$ computations. On the other hand, each trajectory contains n time slots, so, $n.|\mathcal{P} \cup \mathcal{H}|$ computations are needed. Finally, since δ days should be considered by the systems, the total time complexity is $O(n.\delta.|\mathcal{P} \cup \mathcal{H}|)$. □

Theorem 2. *The predictor system works in $O(n.\delta)$ time, for each given individual's trajectory.*

Proof. The predictor system uses the trajectory of an individual at each time slot for all the required days, so the total cost is $O(n.\delta)$ time. □

Although various advanced HMMs and deep-learning approaches can adapt to the current problem's setting, in this paper, a general HMM is used due to keeping the model simple and integrated with the detecting system. In detail, there are multiple reasons that HMM is preferred to other learning approaches, particularly the deep-learning approaches, in this research:

- HMMs are simple to implement, manipulate and customize. Also, they need less computational resources comparing the other learning-based methods,
- The population (and the case study in this research) is not so big and is not so complicated related features to use the other learning and deep learning approaches such as LSTM and RNN. We considered a closed population with a negligible rate of immigration,
- HMMs make the Markovian assumption, that is, we assume the current state depends only on the previous state. So, when our data satisfy this assumption roughly, HMMs might be the preferred method, however, other learning-based approaches might find spurious patterns, and hence overfit,

- With HMMs, the inputs and the outputs have a one-to-one correspondence,
- HMMs are generative models, while deep-learning approaches are primarily discriminative models.

It is worth mentioning that the deep-learning approaches such as RNNs and LSTM networks as well as other advanced variations of HMMs have their interests and advantages for analyzing the sequential data, and we believe that some of the current work limitations can be solved using these methods as well using a different modeling and training features.

4.1. ***Adjusting Covid-19 to the Proposed Systems***

The current Covid-19 pandemic has become the greatest concern of the world. The World Health Organization (WHO) reported 95.85 million people around the world have been infected, and unfortunately more than two million people have passed away due to Covid-19 (https://www.worldometers.info/coronavirus/). Therefore, it is the most major pandemic disease in the world, so we adjust the proposed systems to the known properties of this disease and available information in the scientific reports in this concern. We initialize effective parameters on the transmission of Covid-19. Although there are several transmission ways for Covid-19. We adjust all of the impression factors in batches, e.g., using masks and sanitary gloves, methanol for disinfection can be considered as a hygiene parameter in the model.

$$\mathcal{A}_P(p) = (1 - \sigma) \times \beta^d, \tag{8}$$

where σ is the percent of personal hygiene and β is being patient ratio, so β^d is the possibility of being patient in d-th day. Note that, it is assumed the starting day of being patient is unrecognizable. Also, each healthy individual effects the current place hazard rate by:

$$\mathcal{R}_P(p) = 1 + \ln(\sigma)/C, \tag{9}$$

$$\mathcal{G}_P(m) = (1 - \sigma) \times \gamma \times o, \tag{10}$$

where γ is the social distance impact probability, and o is some (probably) missed effective parameters in Covid-19 infection . In the next section, we will verify the accuracy and performance of the proposed approach on Covid-19 initialization.

5. Simulation Results

To validate and analyze the presented detector and predictor systems' performance, we implemented them and conducted a set of experiments on Covid-19. The source codes are available at https:/github.com/mohsen-ghaffari1992/DETECTOR_and_PREDICTOR_SYSTEMS. Since Covid-19 is a currently emerged disease, unfortunately, there is no complete real data set that contains all the parameters introduced in this study. So, we used real data as much as possible and generated the missed data by applying real-world's features to be more reliable. We will explain the way of providing data and all the initialization of the parameters in the following.

As aforementioned, the input of the detector system is a graph of a specific city and the trajectories of people who live in the city. We studied Sareyn city (Figure 1a), a small city in the north-west of Iran which we have its graph and high-risk and infected places as well as most parameters of the models based on the local experts' reports. This city contains about 2500 buildings, markets and stores, gas stations, bus and taxi stations (during the studies the schools, restaurants, gyms, hairdresser and fashion stores were closed), and about 7000 population which 183 of them allow us to access their movements' trajectory partially. We assumed each floor of a building as an independent node in the graph, and the node that corresponds to the ground floor connects other nodes of the building to outer nodes. First, we construct the corresponding graph of the city (includes 5000 nodes) and label each node with a random value that shows the number of people who could be there at the moment. Then, we make

trajectories by using *random walking* on the weighted graph. We control random walking in the city by using gathered information for the group of volunteers, such a way that each person is at home from 00:00 until 07:00, then he/she go out for a while (that is random between 7 to 14 hours) and go back home. Also, each time slot in this simulation is 10 minutes, and people do not have a connection along the path. Without loss of generality, we suppose that the latent period of Covid-19 is two days ($\delta = 2$), and $\beta = 0.8$ (see Eq. (8)).

To validate the detector system, we utilize experts' reports to determine the hazardous rate of each place. Then, we run the predictor system for a group of people and obtain the possibility of being infected for each person. Next, we put them into two categories; the healthy (the individuals whose patient possibility is less than 50%) and the patients (the individuals whose patient possibility is equal or more than 50%). In this part, we use a set of volunteer individuals' data (without knowing their ID) and a set of random trajectories. Finally, we consider the trajectories of these people as the input of the detector system. In this case, we expect that the system is able to find the hazard places determined by the expert.

Figure 5 Schematic illustration of comparison between defined information by the expert (a), and the detector system's results (b).

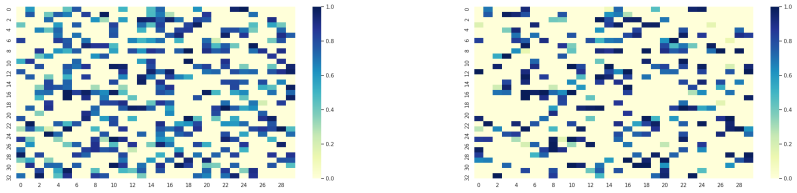

(a) **(b)**

Figure 5 displays the results of the first round of the simulations. Also, the details of the results are presented in Table A.6 in the Appendix. As it can be seen in Figure 5, the proposed detector system can find the infected places with high probability, however, there are still some places that are not detected

by the system. This happens because the population did not visit those places sufficiently to learn. So, if the required data was available in the real world, the proposed system could detect the hazardous rate of the places. Note that, the illustrated nodes in Figure 5 are ordered based on their index, and their corresponding places in the city are not neighbors necessarily.

Now, we study the information provided by the layered structure in analyzing people treatment. Figure 6 and Figure 7 illustrate layers corresponds with four 30-minutes intervals and four daily intervals, respectively. Comparing the obtained results with the information presented by the experts, it is confirmed that the detector system works well most of the time. So that, it detects 72% of hazardous places, and for 28% of places which it cannot detect, the average of the hazard ratio is 61%. On the other hand, it makes a mistake for 1% places and detects safe places as hazardous places. This error happens due to a lack of real data, and one way to overwhelm this issue is that more individuals participate in gathering data particularly the infected individuals. Also, as expected, we observed the hazard ratio of the places changes smoothly in a day.

In general, each person has almost stable and iterative movement trajectories in a period of time. So, we expect that the hazardous ratio does not change suddenly in a period like a few consecutive days. Figure 7 shows a significant difference in the hazardous ratio of a specific place on different days. The main reason for this is the lack of real-world data, however, by incorporating the experts' knowledge in initializing rates of the places this problem can be smoothed. The initializing period problem corresponds to the first day of input trajectories. So, the detector system assumes almost no foreknowledge of the hazardous rates. Particularly, this happens in the first time intervals, and after passing some time intervals what is learned by the detector system closes to the true information.

To validate the predictor system, we choose individuals with the known diagnostic test result and compare the output of the system with them. We assume $C = 1$ in Eq. (9) in the simulations. According to the results, the predictor system is 96% successful in predicting the disease. However, the test

also yields a false-positive result for 1% of healthy people. For a prevalence rate of 10%, the probability of an individual has truly the disease given his/her predictor test result is positive is computed by the following:

$$\begin{aligned}\rho(p|T_+) &= \frac{\rho(p \cap T_+)}{\rho(T_+)} \\ &= \frac{\rho(T_+|p)\rho(p)}{\rho(T_+|p)\rho(p) + \rho(T_+|h)\rho(h)} \\ &= \frac{(0.96)(0.1)}{(0.96)(0.1) + (0.01)(0.9)} \\ &\simeq 91.4\%\end{aligned} \tag{11}$$

Next, we investigate the sensitivity analyzes of them. We considered all the parameters in three batches. Table 2 illustrates the impact of hygiene on hazardous places and the possibility of being infected with Covid-19. According to these results, if all the people of a city respect personal hygiene more than 80%, all places will be safe with high probability. Accordingly, personal hygiene can resist the propagation of infectious diseases.

Table 2 Impact of the hygiene parameter on the environment when the tests are applied on the people who do not diagnostic tests

Hygiene percent	The number of patients	The number of healthy individuals	The number of places with at least 60% hazardous	The number of places with at least 80% hazardous	The number of places with at least 90% hazardous
0-10	843	157	523	389	303
10-20	712	288	433	312	267
20-30	691	309	361	193	178
30-40	689	311	229	54	34
40-50	666	334	197	54	25
50-60	592	408	112	38	21
60-70	508	492	87	6	9
70-80	148	852	52	3	1
80-90	0	1000	36	3	0
90-100	0	1000	14	2	0

The importance of social distance is less than the personal hygiene parameter, but it is an important parameter to decrease the possibility of the Covid-19 outbreak. The impact of social distance studies in Table 3, which illustrates disregarding that may increase the possibility of being infected. According to

the results, decreasing the social distance would be enough reason for highly spreading infectious disease.

Table 3 Impact of the social distance parameter on the environment

Social distance impact ratio	The number of patients	The number of healthy individuals	The number of places with at least 60% hazardous	The number of places with at least 80% hazardous	The number of places with at least 90% hazardous
0.05	486	514	351	212	134
0.1	598	402	351	212	134
0.2	705	295	351	212	134

In addition to personal hygiene and social distance, other influential parameters such as touching a surface (Santarpia et al., 2020) and temperature (Riddell et al., 2020) affect on spreading Covid-19. Unfortunately, there is no precise and reliable information in this regard for Covid-19. For this reason, we consider a batch of such parameters includes parameters whose impacts are unknown. The results are presented in Table 4. In comparison with Table 3, it is clarified that sometimes such unknown parameters are influential than the social distance parameter because it contains a batch of effective transmission parameters.

Table 4 Impact of other effective parameters on the environment

Impact ratio	The number of patients	The number of healthy individuals	The number of places with at least 60% hazardous	The number of places with at least 80% hazardous	The number of places with at least 90% hazardous
0.05	503	497	351	212	134
0.1	607	393	351	212	134
0.2	675	325	351	212	134

Since we are not sure about our knowledge of the Covid-19 transmission functions, we have to investigate the accuracy of it for different accuracy rate of healthy individuals, C. It would get different values for different environments and determining an exact value is difficult. On the other hand, C may change over time. We study it in Table 5. The value of C=1 is the best one for the environment in our case study. Note that, lack of exact information about the infectious disease can lead the proposed systems to weak results.

Table 5 Impact of accuracy rate of the healthy individuals, C

C	Patient detecting	Healthy detecting
1	96%	91.6%
2	96%	91%
3	96%	89%
4	95%	83%
5	95%	82%
6	94%	81.8%
7	93%	81.2%
8	93%	81%
9	92%	80%
10	91%	79.2%

6. Conclusion

The importance of infectious diseases and pandemics in all aspect of human life is clear for all. The Coronavirus disease (COVID-19) is a nowadays example of such pandemics. Finding an approach to decrease such disease exposure, and help to efficiently manage them, is tangible. In this paper, we developed simple and efficient systems to detect the hazardous places of the contagious disease in a city and predict the patient possibility of individuals. Our approach is based on the hidden Markov model and learns and works by applying movement trajectories of patients and healthy individuals around an environment. The proposed approaches are generalized frameworks and can be simply applied to any infectious disease by adjusting corresponding parameters. We applied the Covid-19 setting and verified the approach using a small city's individuals regarding the available information. The results showed that the error rate for predicting the patient possibility in the predictor system is highly acceptable in comparison to the diagnostic test. The results also illustrate that the detector system can detect the hazardous rate of each place. That is useful for giving a warning about the risks of places to care more.

Excessive dependence on data is the major problem of this research, which lack of data can decrease the accuracy of the systems. This issue will be more tangible when some people do not allow us to gather their daily trajectories. Besides, the influential factors and their impact are not available at first. For this reason, both systems can result in unreliable answers. To overcome these prob-

lems, finding an approach that works based on the gathered data i.e. satellite images seems helpful.

In general, we believe the results of this study can be used to establish on time and proper rules and protocols for efficiently managing and controlling disease spreading. We avoid designing complex systems with many parameters and keep the model and the detector and predictor systems simple as much as possible. We showed that the history of individuals' locations can considerably help in detecting infected places and individuals. Testing and verifying the proposed systems by applying them to more case studies with available disease parameters is an extension of this study. Also, using much more complex and deep learning approaches such as long short-term memory can be mentioned as another extension.

Acknowledgement

The authors would like to thank the people in Sareyn city who have participated in this project voluntarily and let their movement trajectory as well as their diagnostic test results are available.

References

Ahamad, M., Aktar, S., Rashed-Al-Mahfuz Uddin, S., Lió, P., Xu, H., Summers, M., Quinn, J., & Moni, M. (2020). A machine learning model to identify early stage symptoms of sars-cov-2 infected patients. *Expert Systems with Applications*, . doi:10.1016/j.eswa.2020.113661.

Alaa, A. M., & Schaar, M. V. D. (2018). Forecasting individualized disease trajectories using interpretable deep learning, . doi:arXiv:1810.10489.

Alaa, A. M., & Schaar, M. V. D. (2019). Attentive state-space modeling of disease progression. *33rd Conference on Neural Information Processing Systems*, .

Apostolopoulos, I. D., & Mpesiana, T. A. (2020). Covid-19: automatic detection from x-ray images utilizing transfer learning with convolutional neural networks. *Physical and Engineering Sciences in Medicine*, . doi:10.1007/s13246-020-00865-4.

Atkeson, A. (2020). What will be the economic impact of covid-19 in the us? rough estimates of disease scenarios. *National Bureau of Economic Research*, *26867*. doi:10.3386/w26867.

Bashir, F., Wei, Q., Khokhar, A., & Schonfeld, D. (2005). Hmm-based motion recognition system using segmented pca. *IEEE International Conference on Image Processing*, . doi:10.1109/icip.2005.1530635.

Bueno, M. L. P., Hommersom, A., Lucas, P. J. F., & Janzing, J. (2019). A probabilistic framework for predicting disease dynamics: a case study of psychotic depression. *Journal of Biomedical Informatics*, . doi:10.1016/j.jbi.2019.103232.

Choudhury, R., Barrett, C. D., Moore, H. B., Moore, E. E., McIntyre, R. C., Moore, P. K., Talmor, D. S., Nydam, T. L., & Yaffe, M. B. (2020). Salvage use of tissue plasminogen activator (tpa) in the setting of acute respiratory distress syndrome (ards) due to covid-19 in the usa: a markov decision analysis. *World Journal of Emergency Surgery*, *15(1)*. doi:10.1186/s13017-020-00305-4.

Chumachenko, D., Meniailov, I., Bazilevych, K., Chumachenko, T., & Yakovlev, S. (2022). Investigation of statistical machine learning models for covid-19 epidemic process simulation: Random forest, k-nearest neighbors, gradient boosting. *Computation*, *10*. URL: https://www.mdpi.com/2079-3197/10/6/86. doi:10.3390/computation10060086.

Davoodi, M., & Ghaffari, M. (2021). Shortest path problem on uncertain networks: An efficient two phases approach. *Computers & Industrial Engineering*, *157*, 107302. doi:https://doi.org/10.1016/j.cie.2021.107302.

Escobar, M., Jeanneret, G., Bravo-Sánchez, L., Castillo, A., Gómez, C., Valderrama, D., Roa, M. F., Martínez, J., Madrid-Wolff, J., Cepeda, M. et al. (2020). Smart pooling: Ai-powered covid-19 testing. *medRxiv*, .

Fong, S. J., Li, G., Dey, N., Crespo, R. G., & Herrera-Viedma, E. (2020). Composite monte carlo decision making under high uncertainty of novel coronavirus epidemic using hybridized deep learning and fuzzy rule induction. *Applied Soft Computing Journal*, . doi:10.1016/j.asoc.2020.106282.

Futoma, J., Sendak, M., Cameron, B., & Heller, K. A. (2016). Scalable joint modeling of longitudinal and point process data for disease trajectory prediction and improving management of chronic kidney disease. *UAI*, .

Galagali, N., & Xu-Wilson, M. (2018). Patient subtyping with disease progression and irregular observation trajectories, . doi:arXiv:1810.09043.

Ghaffari, M., & Afsharchi, M. (2020). Learning to shift load under uncertain production in the smart grid. *International Transactions on Electrical Energy Systems*, *31*. doi:10.1002/2050-7038.12748.

Gozes, O., Frid-Adar, M., Greenspan, H., Browning, P. D., Zhang, H., Ji, W., Bernheim, A., & Siegel, E. (2020). Rapid ai development cycle for the coronavirus (covid-19) pandemic: Initial results for automated detection & patient monitoring using deep learning ct image analysis. *arXiv, Electrical Engineering and Systems Science*, . doi:arXiv:2003.05037.

Hernandez-Matamoros, A., Fujita, H., Hayashi, T., & Perez-Meana, H. (2020). Forecasting of covid19 per regions using arima models and polynomial functions. applied soft computing. *Applied Soft Computing Journal*, . doi:10.1016/j.asoc.2020.106610.

Irio, L., & Oliveira, R. (2021). A comparative evaluation of probabilistic and deep learning approaches for vehicular trajectory prediction. *IEEE Open Journal of Vehicular Technology*, *2*, 140–150. doi:10.1109/OJVT.2021.3063125.

Ismael, A., & Şengür, A. (2020). Deep learning approaches for covid-19 detection based on chest x-ray images. *Expert Systems with Applications*, . doi:https://doi.org/10.1016/j.eswa.2020.114054.

Kim, J., Singh, S., Thiessen, E. D., & Fisher, A. V. (2020). A hidden markov model for analyzing eye-tracking of moving objects. *Behavior Research Methods*, . doi:10.3758/s13428-019-01313-2.

Kumar, K. N. (2020). Analyzing cursor movements with an hmm to assess individual differences in cognition reliably and quickly. *ProQuest*, .

Li, L., Qin, L., Xu, Z., Yin, Y., Wang, X., Kong, B., Bai, J., Lu, Y., Fang, Z., Song, Q., Cao, K., Liu, D., Wang, G., Xu, Q., Fang, X., Zhang, S., Xia, J., & Xia, J. (2020a). Artificial intelligence distinguishes covid-19 from community acquired pneumonia on chest ct. *RSNA*, . doi:10.1148/radiol.2020200905.

Li, S., Wang, Y., Xue, J., Zhao, N., & Zhu, T. (2020b). The impact of covid-19 epidemic declaration on psychological consequences: A study on active weibo users. *International Journal of Environmental Research and Public Health*, *17(6)*, 2032. doi:10.3390/ijerph17062032.

Lim, B., & Schaar, M. V. D. (2018). Disease-atlas: Navigating disease trajectories using deep learning, . doi:arXiv:1803.10254.

Liu, Y., Gayle, A. A., Wilder-Smith, A., & Rocklov, J. (2020). The reproductive number of covid-19 is higher compared to sars coronavirus. *Journal of Travel Medicine*, . doi:10.1093/jtm/taaa021.

Mutesa, L., Ndishimye, P., Butera, Y., Souopgui, J., Uwineza, A., Rutayisire, R., Ndoricimpaye, E. L., Musoni, E., Rujeni, N., Nyatanyi, T. et al. (2020). A pooled testing strategy for identifying sars-cov-2 at low prevalence. *Nature*, (pp. 1–5).

Nagesh, S., Moreno, A., Ishikawa, H., Wollstein, G., Schuman, J. S., & Rehg, J. M. (2019). A spatiotemporal approach to predicting glaucoma progression using a ct-hmm. *Machine Learning for Healthcare*, *106*, :1–19.

Neyja, M., Mumtaz, S., Huq, K. M. S., Busari, S. A., Rodriguez, J., & Zhou, Z. (2017). An iot-based e-health monitoring system using ecg signal. *IEEE Global Communications Conference*, . doi:10.1109/glocom.2017.8255023.

Ong, E., Wong, M. U., Huffman, A., & He, Y. (2020). Covid-19 coronavirus vaccine design using reverse vaccinology and machine learning. *National Institute of Health*, . doi:10.1101/2020.03.20.000141.

Perez, L., & Dragicevic, S. (2009). An agent-based approach for modeling dynamics of contagious disease spread. *International Journal of Health Geographics*, *8(50)*. doi:10.1186/1476-072X-8-50.

Pham, T., Tran, T., Phung, D., & Venkatesh, S. (2017). Predicting healthcare trajectories from medical records: A deep learning approach. *Journal of Biomedical Informatics*, *69*, 218–229. doi:10.1016/j.jbi.2017.04.001.

Priyanka, Kumari, A., & Sood, M. (2021). Implementation of simplernn and lstms based prediction model for coronavirus disease (covid-19). *IOP Conf. Ser.: Mater. Sci. Eng.*, *1022*. doi:10.1088/1757-899X/1022/1/012015.

Randhawa, G. S., Soltysiak, M. P. M., El Roz, H., de Souza, C. P. E., Hill, K. A., & Kari, L. (2020). Machine learning using intrinsic genomic signatures for rapid classification of novel pathogens: Covid-19 case study. *PLOS ONE*, *15(4)*. doi:10.1371/journal.pone.0232391.

Rao, A. S. R. S., & Vazquez, J. A. (2020). Identification of covid-19 can be quicker through artificial intelligence framework using a mobile phone-based survey in the populations when cities/towns are under quarantine. *Infection Control & Hospital Epidemiology*, (pp. 1–18). doi:10.1017/ice.2020.61.

Riddell, S., Goldie, S., Hill, A., Eagles, D., & Drew, T. W. (2020). The effect of temperature on persistence of sars-cov-2 on common surfaces. *Virology journal*, *17*, 1–7.

Roda, W. C., Varughese, M. B., Han, D., & Li, M. Y. (2020). Why is it difficult to accurately predict the covid-19 epidemic? *Infectious Disease Modelling*, . doi:10.1016/j.idm.2020.03.001.

Saini, R., Kumar, P., Roy, P. P., & Pal, U. (2020). Trajectory classification using feature selection by genetic algorithm. *Advances in Intelligent Systems and Computing*, *1024(2)*, 377–388.

Santarpia, J. L., Rivera, D. N., Herrera, V. L., Morwitzer, M. J., Creager, H. M., Santarpia, G. W., Crown, K. K., Brett-Major, D. M., Schnaubelt, E. R., Broadhurst, M. J. et al. (2020). Aerosol and surface contamination of sars-cov-2 observed in quarantine and isolation care. *Scientific reports*, *10*, 1–8.

Tian, Y., & Zhang, I. L. X. (2020). Forecasting covid-19 cases using machine learning models. *33rd Conference on Neural Information Processing Systems (NeurIPS 2019), Vancouver, Canada*, . doi:10.1101/2020.07.02.20145474.

Vairavan, S., Eshelman, L., Haider, S., Flower, A., & Seiver, A. (2012). Prediction of mortality in an intensive care unit using logistic regression and a hidden markov model. *Computing in Cardiology*, (pp. 393–396).

Wang, S., Kang, B., Ma, J., Zeng, X., Xiao, M., Guo, J., Cai, M., Yang, J., Li, Y., Meng, X., & Xu, B. (2020). A deep learning algorithm using ct images to screen for corona virus disease (covid-19), . doi:10.1101/2020.02.14.20023028.

Wang, Y., Yan, Z., Wang, D., Yang, M., Li, Z., Gong, X., Wu, D., Zhai, L., Zhang, W., & Wang, Y. (2022). Prediction and analysis of covid-19 daily new cases and cumulative cases: times series forecasting and

machine learning models. *BMC Infectious Diseases*, *495*. doi:10.1186/s12879-022-07472-6.

Wynants, L., Van Calster, B., Bonten, M. M. J., Collins, G. S., Debray, T. P. A., De Vos, M., Haller, M. C., Heinze, G., Moons, K. G. M., Riley, R. D., Schuit, E., Smits, L. J. M., Snell, K. I. E., Steyerberg, E. W., Wallisch, C., & van Smeden, M. (2020). Prediction models for diagnosis and prognosis of covid-19 infection: systematic review and critical appraisal. *BMJ*, . doi:10.1136/bmj.m1328.

Xiang, J., Soon, A. C., Geller, J., & Oria, V. (2015). Collaborative and trajectory prediction models of medical conditions by mining patients' social data. *IEEE International Conference on Bioinformatics and Biomedicine*, . doi:10.1109/bibm.2015.7359771.

Yan, L., Zhang, H. T., Xiao, Y., Wang, M., Guo, Y., Sun, C., Tang, X., Jing, L., Li, S., Zhang, M., Xiao, Y., Cao, H., Chen, Y., Ren, T., Jin, J., Wang, F., Xiao, Y., Huang, S., Tan, X., Huang, N., Jiao, B., Zhang, Y., Luo, A., Cao, Z., Xu, H., & Yuan, Y. (2020). Prediction of criticality in patients with severe covid-19 infection using three clinical features: a machine learning-based prognostic model with clinical data in wuhan, . doi:10.1101/2020.02.27.20028027.

Appendix A. Validating the detector system

Table A.6: Comparison between a complete layer of $\mathcal{S}$ and corresponding layer information defined by expert.

Expert	Detector	Expert	Detector	Expert	Detector	Expert	Detector	Expert	Detector
0.0	0.0	0.6	0.69	0.0	0.0	0.0	0.0	0.0	0.0
0.43	0.93	0.77	0.0	0.0	0.0	0.0	0.0	0.0	0.0
0.0	0.0	0.5	0.0	0.0	0.0	0.0	0.0	0.47	0.09
0.73	0.73	0.0	0.0	0.0	0.0	0.0	0.0	0.62	0.46
0.0	0.0	0.0	0.0	0.0	0.0	0.96	0.96	1.0	0.98
0.0	0.0	0.0	0.0	0.0	0.0	0.0	0.0	0.0	0.0
0.0	0.0	0.76	0.76	0.0	0.0	0.41	0.98	0.75	0.94
0.67	0.79	0.0	0.0	0.84	0.0	0.0	0.0	0.99	0.78
0.0	0.0	0.0	0.0	0.0	0.0	0.0	0.0	0.48	0.62
0.68	0.68	0.29	0.29	0.0	0.0	0.0	0.0	0.0	0.0
0.86	0.0	0.0	0.0	0.0	0.0	0.0	0.0	0.0	0.0
0.71	0.0	0.0	0.0	0.0	0.0	0.0	0.0	0.0	0.0
0.0	0.0	0.0	0.0	0.0	0.0	0.72	0.0	0.0	0.0
0.0	0.0	0.0	0.0	0.0	0.0	0.62	0.41	0.32	0.39
0.0	0.0	0.58	0.0	0.0	0.0	0.96	0.99	0.94	0.8
0.77	0.0	0.96	0.96	0.7	0.97	0.0	0.0	0.81	0.0
0.77	0.69	0.0	0.0	0.0	0.0	0.0	0.0	0.0	0.0
0.0	0.0	0.0	0.0	0.9	0.0	0.0	0.0	0.0	0.0
0.42	0.18	0.0	0.0	0.0	0.0	0.0	0.0	0.59	0.0
0.0	0.0	0.75	0.94	0.0	0.0	0.0	0.0	0.0	0.0
0.83	0.0	0.0	0.0	0.0	0.0	0.72	0.0	0.45	0.84
0.83	0.97	0.0	0.0	0.0	0.0	0.83	0.97	0.98	0.98
0.0	0.0	0.0	0.0	0.0	0.0	0.0	0.0	0.0	0.0
0.46	0.15	0.0	0.0	0.56	0.0	0.4	0.0	0.0	0.0
0.0	0.0	0.0	0.0	0.65	0.0	0.43	0.38	0.73	0.93
0.0	0.0	0.0	0.0	0.0	0.0	0.0	0.0	0.0	0.0
0.76	0.0	0.0	0.0	0.0	0.0	0.51	0.62	0.0	0.0
0.77	0.0	0.0	0.0	0.83	0.83	0.85	0.0	0.0	0.0
0.0	0.0	0.0	0.0	0.79	0.79	0.8	0.0	0.7	0.0
0.39	0.0	0.0	0.0	0.0	0.0	0.73	0.73	0.0	0.0
0.0	0.0	0.0	0.0	0.0	0.0	0.0	0.0	0.7	0.7
0.0	0.0	0.7	0.7	0.0	0.0	0.0	0.0	0.0	0.0
0.78	0.78	0.0	0.0	0.0	0.0	0.0	0.0	0.0	0.0
0.0	0.0	0.77	0.81	0.93	0.93	0.0	0.0	0.0	0.0
0.0	0.0	0.0	0.0	0.96	0.97	0.0	0.0	0.86	0.86
0.0	0.0	0.0	0.0	0.0	0.0	0.9	0.9	0.75	0.85
0.84	0.84	0.0	0.0	0.0	0.0	0.0	0.0	0.85	0.85
0.76	0.76	0.0	0.0	0.7	0.91	0.0	0.0	0.0	0.0
0.0	0.0	0.0	0.0	0.66	0.79	0.5	0.5	0.59	0.68
0.71	0.71	0.0	0.0	0.5	0.0	0.0	0.0	0.0	0.0
0.72	0.62	0.22	1.0	0.0	0.0	0.0	0.0	0.0	0.0
0.0	0.0	0.0	0.0	0.4	0.13	0.79	0.0	0.0	0.0
0.0	0.0	0.0	0.0	0.0	0.0	0.0	0.0	0.0	0.0
0.78	0.99	0.0	0.0	0.94	0.0	0.87	0.0	0.87	0.87
0.48	0.38	0.0	0.0	0.0	0.0	0.0	0.0	0.0	0.0
0.0	0.0	0.0	0.0	0.0	0.0	0.0	0.0	0.0	0.0
0.81	0.81	0.48	0.48	0.75	0.69	0.41	0.41	0.0	0.0
0.99	0.98	0.0	0.0	0.0	0.0	0.0	0.0	0.0	0.0
0.0	0.0	0.0	0.0	0.86	0.0	0.0	0.0	0.61	0.63

Continued on next page

Table A.6 – continued from previous page

Expert	Detector	Expert	Detector	Expert	Detector	Expert	Detector	Expert	Detector
0.52	0.14	0.75	0.0	0.0	0.0	0.0	0.0	0.0	0.0
0.57	0.43	0.0	0.0	0.8	0.0	0.61	0.92	0.88	0.88
0.82	0.97	0.0	0.0	0.75	0.0	1.0	0.99	0.0	0.0
0.9	0.9	0.75	0.75	0.81	0.81	0.0	0.0	0.0	0.0
0.71	0.71	0.89	1.0	0.0	0.0	0.9	0.99	0.0	0.0
0.0	0.0	0.0	0.0	0.42	0.54	0.62	1.0	0.0	0.0
0.0	0.0	0.0	0.0	0.0	0.0	0.62	0.0	0.77	0.77
0.0	0.0	0.0	0.0	0.0	0.0	0.0	0.0	0.0	0.0
0.0	0.0	0.0	0.0	0.0	0.0	0.0	0.0	0.0	0.0
0.0	0.0	0.0	0.0	0.0	0.0	0.0	0.0	0.0	0.0
0.0	0.0	0.0	0.0	0.87	0.0	0.0	0.0	0.0	0.0
0.52	0.0	0.86	0.0	0.0	0.0	0.0	0.0	0.0	0.0
0.0	0.0	0.73	0.73	0.0	0.0	0.0	0.0	0.0	0.0
0.0	0.0	0.0	0.0	0.0	0.0	0.58	0.42	0.85	0.0
0.0	0.0	0.0	0.0	0.0	0.0	0.99	0.95	0.0	0.0
0.0	0.0	0.0	0.0	0.89	0.99	0.0	0.0	0.0	0.0
0.0	0.0	0.0	0.0	0.0	0.0	0.88	0.0	0.0	0.0
0.0	0.0	0.0	0.0	0.79	0.96	0.0	0.0	0.0	0.0
0.77	0.0	0.7	0.91	0.87	0.0	0.0	0.0	0.0	0.0
0.98	1.0	0.96	0.81	0.0	0.0	0.0	0.0	0.81	1.0
0.0	0.0	0.0	0.0	0.0	0.0	0.0	0.0	0.74	0.74
0.83	0.83	0.0	0.0	0.82	0.82	0.0	0.0	0.38	0.98
0.0	0.0	0.0	0.0	0.42	0.2	0.0	0.0	0.95	0.94
0.77	1.0	0.0	0.0	0.0	0.0	0.0	0.0	0.0	0.0
0.72	0.92	0.0	0.0	0.0	0.0	0.0	0.0	0.0	0.0
0.0	0.0	0.88	0.88	0.0	0.0	0.0	0.0	0.95	0.82
0.72	0.64	0.96	1.0	0.0	0.0	0.0	0.0	0.0	0.0
0.7	0.72	0.73	0.73	0.0	0.0	0.8	0.0	0.71	0.83
0.73	0.0	0.0	0.0	0.77	0.77	0.89	0.0	0.97	1.0
0.0	0.0	0.75	0.0	0.0	0.0	0.39	0.0	0.0	0.0
0.51	0.99	0.0	0.0	0.85	0.85	0.0	0.0	0.0	0.0
0.0	0.0	0.66	0.47	0.0	0.0	0.95	0.99	0.68	0.94
0.0	0.0	0.84	0.84	0.66	0.0	0.54	0.7	0.0	0.0
0.0	0.0	0.0	0.0	0.0	0.0	0.0	0.0	0.0	0.0
0.0	0.0	0.0	0.0	0.0	0.0	0.0	0.0	0.0	0.0
0.0	0.0	0.0	0.0	0.0	0.0	0.82	0.82	0.0	0.0
0.74	0.93	0.0	0.0	0.0	0.0	0.0	0.0	0.0	0.0
0.81	0.64	0.0	0.0	0.0	0.0	0.97	0.85	0.0	0.0
0.89	0.89	0.0	0.0	0.0	0.0	0.0	0.0	0.0	0.0
0.0	0.0	0.0	0.0	0.82	0.82	0.81	0.0	0.75	0.94
0.0	0.0	0.8	0.8	0.0	0.0	0.66	0.67	0.0	0.0
0.0	0.0	0.0	0.0	0.36	0.22	0.81	0.96	0.78	0.0
0.73	0.0	0.0	0.0	0.0	0.0	0.31	0.24	0.0	0.0
0.0	0.0	0.33	0.6	0.0	0.0	0.0	0.0	0.0	0.0
0.74	0.0	0.88	0.99	0.0	0.0	0.0	0.0	0.0	0.0
0.0	0.0	0.0	0.0	0.0	0.0	0.82	0.82	0.0	0.0
0.0	0.0	0.52	0.53	0.45	0.0	0.0	0.0	0.98	0.0
0.0	0.0	0.0	0.0	0.7	0.7	0.72	0.72	0.0	0.0
0.99	1.0	0.84	0.97	0.97	1.0	0.72	0.72	0.64	0.64
0.98	1.0	0.46	0.0	0.0	0.0	0.0	0.0	0.0	0.0
0.79	0.0	0.73	0.84	0.0	0.0	0.0	0.0	0.0	0.0
0.98	0.0	0.49	0.0	0.0	0.0	0.56	0.29	0.64	0.64
0.0	0.0	0.0	0.0	0.7	0.7	0.0	0.0	0.73	0.0
0.0	0.0	0.0	0.0	0.51	0.0	0.0	0.0	0.0	0.0
0.99	1.0	0.0	0.0	0.9	0.9	0.0	0.0	0.68	0.83

Continued on next page

Table A.6 – continued from previous page

Expert	Detector	Expert	Detector	Expert	Detector	Expert	Detector	Expert	Detector
0.0	0.0	0.0	0.0	0.43	0.43	0.0	0.0	0.0	0.0
0.0	0.0	0.0	0.0	0.0	0.0	0.0	0.0	0.79	0.0
0.0	0.0	0.0	0.0	0.0	0.0	0.0	0.0	0.43	0.0
0.0	0.0	0.0	0.0	0.0	0.0	0.0	0.0	0.97	0.97
0.0	0.0	0.0	0.0	0.0	0.0	0.86	0.0	0.0	0.0
0.0	0.0	0.0	0.0	0.0	0.0	0.0	0.0	0.82	0.82
0.83	0.0	0.9	0.0	0.0	0.0	0.0	0.0	0.42	0.0
0.87	0.87	0.75	0.0	0.0	0.0	0.0	0.0	0.0	0.0
0.0	0.0	0.0	0.0	0.71	0.71	0.0	0.0	0.0	0.0
0.69	0.0	0.21	0.16	0.0	0.0	0.85	0.0	0.0	0.0
0.0	0.0	0.74	0.0	0.0	0.0	0.89	0.0	0.0	0.0
0.0	0.0	0.0	0.0	0.0	0.0	0.73	0.58	0.0	0.0
0.0	0.0	0.76	0.94	0.97	0.97	0.96	0.99	0.74	0.0
0.0	0.0	0.56	0.0	0.0	0.0	0.0	0.0	0.0	0.0
0.0	0.0	0.84	0.84	1.0	1.0	0.75	0.94	0.55	0.55
0.63	0.65	0.0	0.0	0.0	0.0	0.0	0.0	0.0	0.0
0.0	0.0	0.0	0.0	0.37	0.0	0.0	0.0	0.0	0.0
0.0	0.0	0.0	0.0	0.9	0.0	0.7	0.91	0.0	0.0
0.0	0.0	0.0	0.0	0.0	0.0	0.0	0.0	0.0	0.0
0.0	0.0	0.64	0.87	0.0	0.0	0.0	0.0	0.0	0.0
0.0	0.0	0.81	0.0	0.0	0.0	0.0	0.0	0.0	0.0
0.0	0.0	0.75	0.0	0.0	0.0	0.0	0.0	0.0	0.0
0.78	0.95	0.0	0.0	0.0	0.0	0.0	0.0	0.0	0.0
0.0	0.0	0.0	0.0	0.93	0.71	0.0	0.0	0.59	0.0
0.8	0.0	0.0	0.0	0.51	0.42	0.0	0.0	0.0	0.0
0.0	0.0	0.0	0.0	0.0	0.0	0.99	0.99	0.45	0.5
0.0	0.0	0.42	0.6	0.0	0.0	0.54	0.0	0.0	0.0
0.0	0.0	0.88	0.88	0.97	1.0	0.0	0.0	0.0	0.0
0.0	0.0	0.99	0.99	0.0	0.0	0.0	0.0	0.75	0.94
0.49	0.0	0.78	0.78	0.0	0.0	0.0	0.0	0.0	0.0
0.81	0.81	0.0	0.0	0.0	0.0	0.0	0.0	0.0	0.0
0.9	0.9	0.0	0.0	0.57	0.57	0.62	0.83	0.82	0.97
0.0	0.0	0.0	0.0	0.62	0.75	0.6	0.0	0.72	0.99
0.0	0.0	0.0	0.0	0.78	0.95	0.0	0.0	0.0	0.0
0.31	0.27	0.77	0.0	0.44	0.65	0.19	0.0	0.0	0.0
0.99	0.99	0.0	0.0	0.0	0.0	0.49	0.49	0.0	0.0
0.0	0.0	0.87	0.98	0.0	0.0	0.0	0.0	0.0	0.0
0.78	0.0	0.72	0.72	0.82	0.0	0.0	0.0	0.88	0.88
0.0	0.0	0.0	0.0	0.0	0.0	0.0	0.0	0.0	0.0
0.81	0.0	0.87	0.0	0.81	0.96	1.0	1.0	0.47	0.61
0.0	0.0	0.0	0.0	0.0	0.0	0.99	0.79	0.73	0.85
0.0	0.0	0.0	0.0	0.0	0.0	0.0	0.0	0.77	0.0
0.0	0.0	0.0	0.0	0.0	0.0	0.74	0.0	0.0	0.0
0.69	0.8	0.0	0.0	0.74	0.74	0.81	0.81	0.0	0.0
0.0	0.0	0.0	0.0	0.8	0.8	0.0	0.0	0.56	0.0
0.0	0.0	0.73	0.93	0.0	0.0	0.0	0.0	0.72	0.72
0.85	0.85	0.4	0.86	0.0	0.0	0.0	0.0	0.35	0.3
0.0	0.0	0.0	0.0	0.0	0.0	0.84	0.97	0.3	0.17
1.0	1.0	0.9	0.9	0.0	0.0	0.0	0.0	0.0	0.0
0.62	0.73	0.56	0.0	0.0	0.0	0.0	0.0	0.0	0.0
0.0	0.0	0.0	0.0	0.95	0.97	0.8	0.0	0.0	0.0
0.0	0.0	0.0	0.0	0.51	0.0	0.0	0.0	0.0	0.0
0.0	0.0	0.62	0.0	0.0	0.0	0.0	0.0	0.0	0.0
0.4	0.2	0.74	0.74	0.0	0.0	0.89	0.99	0.0	0.0
0.46	0.33	0.0	0.0	0.87	0.98	0.0	0.0	0.39	0.0

Continued on next page

Table A.6 – continued from previous page

Expert	Detector	Expert	Detector	Expert	Detector	Expert	Detector	Expert	Detector
0.94	0.0	0.69	0.69	0.0	0.0	0.0	0.0	0.82	0.0
0.53	0.26	0.0	0.0	0.0	0.0	0.0	0.0	0.86	0.86
0.0	0.0	0.0	0.0	0.0	0.0	0.96	0.0	0.0	0.0
0.72	0.98	0.0	0.0	0.0	0.0	0.0	0.0	0.0	0.0
0.0	0.0	0.0	0.0	0.84	0.84	0.89	0.99	0.77	0.9
0.81	0.0	0.0	0.0	0.25	0.0	0.0	0.0	0.0	0.0
0.0	0.0	0.0	0.0	0.57	0.0	0.0	0.0	0.0	0.0
0.0	0.0	0.0	0.0	0.77	0.77	0.0	0.0	0.51	0.64
0.0	0.0	0.0	0.0	0.0	0.0	0.0	0.0	0.0	0.0
0.98	0.85	0.0	0.0	0.82	0.0	0.0	0.0	0.0	0.0
0.0	0.0	0.85	0.5	0.74	0.74	0.0	0.0	0.0	0.0
0.0	0.0	0.81	0.0	0.0	0.0	0.0	0.0	0.0	0.0
0.52	0.0	0.0	0.0	0.92	0.73	0.0	0.0	0.7	0.97
0.0	0.0	0.74	0.74	0.0	0.0	0.83	0.0	0.0	0.0
0.0	0.0	0.0	0.0	0.87	0.98	0.0	0.0	0.88	0.99
0.39	0.65	0.53	0.67	0.0	0.0	0.36	0.0	0.0	0.0
0.0	0.0	0.0	0.0	0.0	0.0	0.0	0.0	0.0	0.0
0.0	0.0	0.7	0.0	0.0	0.0	0.0	0.0	0.59	0.59
0.0	0.0	0.73	1.0	0.0	0.0	0.94	0.95	0.0	0.0
0.94	0.99	0.0	0.0	0.0	0.0	0.0	0.0	0.0	0.0
0.0	0.0	0.0	0.0	0.0	0.0	0.79	0.77	0.78	0.95
0.0	0.0	0.89	0.0	0.0	0.0	0.73	0.73	0.72	0.0
0.0	0.0	0.75	0.0	0.0	0.0	0.0	0.0	0.0	0.0
0.99	1.0	0.86	0.95	0.0	0.0	0.7	0.7	0.0	0.0
0.89	0.0	0.0	0.0	0.99	1.0	0.84	1.0	0.0	0.0
0.4	0.62	0.38	0.0	0.0	0.0	0.74	0.0	0.0	0.0
0.0	0.0	0.0	0.0	0.78	0.62	0.0	0.0	0.46	0.0
0.0	0.0	0.0	0.0	0.82	0.0	0.0	0.0	0.55	0.0
0.98	0.82	0.0	0.0	0.0	0.0	0.45	0.8	0.0	0.0
0.0	0.0	0.49	0.0	0.43	0.42	0.75	0.75	0.0	0.0
0.79	0.79	0.0	0.0	0.0	0.0	0.0	0.0	0.0	0.0
0.73	0.93	0.0	0.0	0.85	0.0	0.0	0.0	0.37	0.46
0.9	0.0	0.0	0.0	0.0	0.0	0.0	0.0	0.0	0.0
0.71	0.0	0.0	0.0	0.98	1.0	0.0	0.0	0.46	0.0
0.89	0.0	0.0	0.0	0.0	0.0	0.85	0.85	0.78	0.0
0.0	0.0	0.0	0.0	0.0	0.0	0.39	0.49	0.0	0.0
0.0	0.0	0.0	0.0	0.0	0.0	0.0	0.0	0.73	0.73
0.66	0.95	0.0	0.0	0.71	0.0	0.95	0.99	0.0	0.0
0.88	0.0	0.0	0.0	0.0	0.0	0.0	0.0	0.0	0.0
0.0	0.0	0.0	0.0	0.0	0.0	0.0	0.0	0.36	0.22
0.6	0.9	0.0	0.0	0.0	0.0	0.86	0.0	0.0	0.0

Figure 6 Comparison between the defined information by the expert (6a) and the detector system's results (6b) from 10:00 until 12:00 on a day.

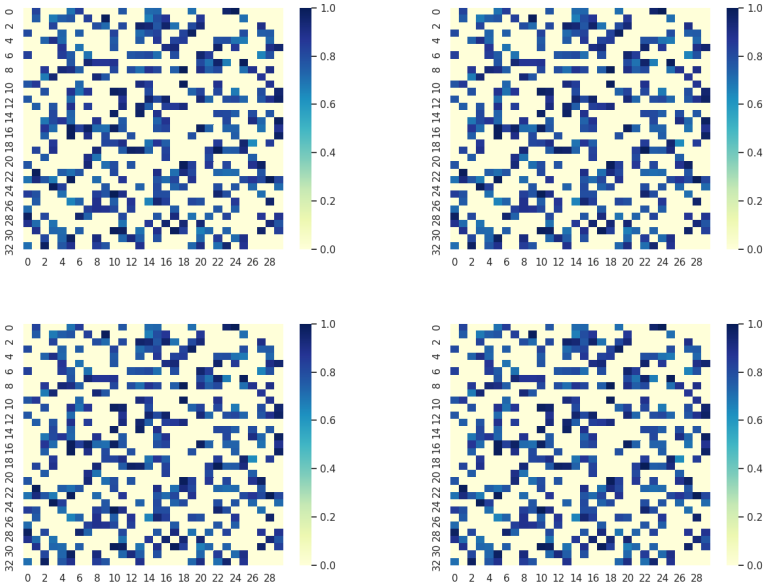

(a)

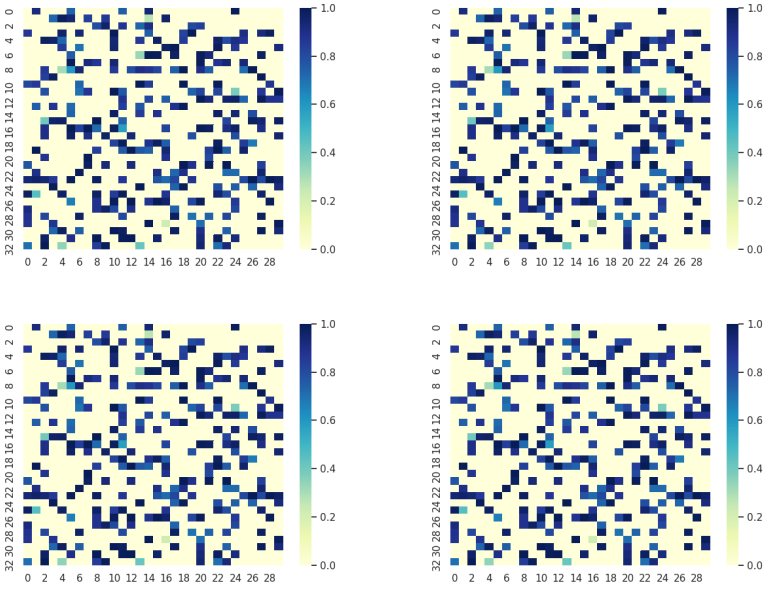

(b)

Figure 7 Comparison between the provided information by expert (7a) and the detector system's results (7b) for four consecutive days at 10:00.

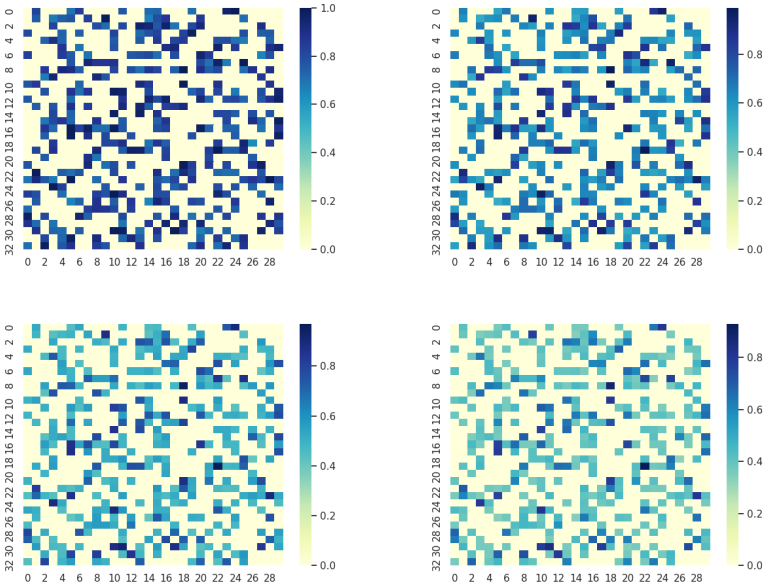

(a)

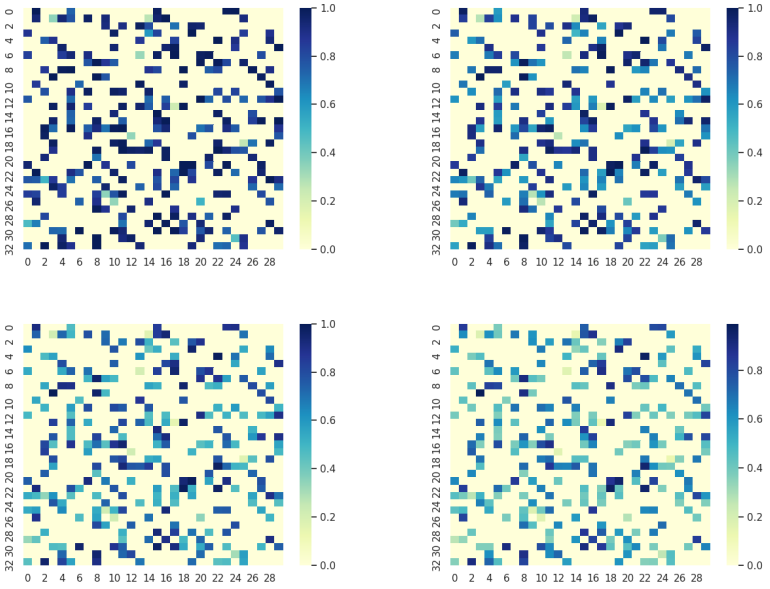

(b)